Strahlenther Onkol (2017) 193:848–855
DOI 10.1007/s00066-017-1165-2

ORIGINAL ARTICLE

Metastasis of breast cancer cells to the bone, lung, and lymph nodes promotes resistance to ionizing radiation

Takamitsu Hara[1] · Manabu Iwadate[2] · Kazunoshin Tachibana[3] · Satoshi Waguri[4] · Seiichi Takenoshita[5] · Nobuyuki Hamada[6]

Received: 6 January 2017 / Accepted: 31 May 2017 / Published online: 22 June 2017

Abstract
Background Metastasis represents the leading cause of breast cancer deaths, necessitating strategies for its treatment. Although radiotherapy is employed for both primary and metastatic breast cancers, the difference in their ionizing radiation response remains incompletely understood. This study is the first to compare the radioresponse of a breast cancer cell line with its metastatic variants and report that such metastatic variants are more radioresistant.
Materials and methods A luciferase expressing cell line was established from human basal-like breast adenocarcinoma MDA-MB-231 and underwent in vivo selections, whereby a cycle of inoculations into the left cardiac ventricle or the mammary fat pad of athymic nude mice, isolation of metastases to the bone, lung and lymph nodes visualized with bioluminescence imaging, and expansion of obtained cells was repeated twice or three times. The established metastatic cell lines were assessed for cell proliferation, wound healing, invasion, clonogenic survival, and apoptosis.
Results The established metastatic cell lines possessed an increased proliferative potential in vivo and were more chemotactic, invasive, and resistant to X-ray-induced clonogenic inactivation and apoptosis in vitro.
Conclusion Breast cancer metastasis to the bone, lung, and lymph nodes promotes radioresistance.

Keywords Breast cancer · Basal subtype · Primary cancer · Metastatic cancer · Radioresistance

Metastasierung von Brustkrebszellen in Knochen, Lunge und Lymphknoten steigert die Resistenz gegenüber ionisierender Strahlung

Zusammenfassung
Hintergrund Metastasierung ist die Hauptursache für den tödlichen Verlauf von Brustkrebserkrankungen. Darauf müssen spezifische Behandlungsstrategien ausgerichtet werden. Sowohl primäre als auch metastatische Brustkrebsarten können mit einer Strahlentherapie behandelt werden, allerdings sind die Unterschiede in der Reaktion auf ionisierende Strahlung bis heute nicht vollständig verstanden. In dieser Studie wird zum ersten Mal die Strahlenantwort

Electronic supplementary material The online version of this article (doi: 10.1007/s00066-017-1165-2) contains supplementary material, which is available to authorized users.

✉ Nobuyuki Hamada
hamada-n@criepi.denken.or.jp

[1] Department of Radiological Technology, School of Radiological Technology, Gunma Prefectural College of Health Sciences, 1-323 Kamioki, Maebashi, Gunma 371-0052, Japan

[2] Department of Thyroid and Endocrinology, School of Medicine, Fukushima Medical University, 1 Hikarigaoka, Fukushima 960-1295, Japan

[3] Department of Breast Surgery, School of Medicine, Fukushima Medical University, 1 Hikarigaoka, Fukushima 960-1295, Japan

[4] Department of Anatomy and Histology, School of Medicine, Fukushima Medical University, 1 Hikarigaoka, Fukushima 960-1295, Japan

[5] Advanced Clinical Research Center, Fukushima Global Medical Science Center, School of Medicine, Fukushima Medical University, 1 Hikarigaoka, Fukushima 960-1295, Japan

[6] Radiation Safety Research Center, Nuclear Technology Research Laboratory, Central Research Institute of Electric Power Industry (CRIEPI), 2-11-1 Iwado-kita, Komae, Tokyo 201-8511, Japan

einer Brustkrebszelllinie mit der ihrer metastatischen Varianten verglichen und die erhöhte Strahlenresistenz der metastatischen Varianten gezeigt.

Material und Methoden Eine Luciferase-exprimierende Zelllinie wurde aus humanen basaloiden Brustadenokarzinomen MDA-MB-231 etabliert und in zwei oder drei Zyklen in vivo selektiert. Dabei wurden die Zellen entweder in den linken Herzventrikel oder in das Fettgewebe der Brust athymischer Nacktmäuse inokuliert. Die durch Biolumineszenz sichtbar gemachten Metastasen wurden aus Knochen, Lunge und Lymphknoten isoliert und expandiert. Die etablierten metastatischen Zelllinien wurden auf Zellproliferation, Wundheilung, Invasion, Klonüberleben und Apoptose getestet.

Ergebnisse Die etablierten metastatischen Zelllinien wiesen in vivo ein gesteigertes proliferatives Potenzial auf. In vitro zeigten sie erhöhte chemotaktische und invasive Aktivität, zudem besaßen sie eine erhöhte Resistenz gegen röntgenstrahleninduzierte klonogene Inaktivierung und Apoptose.

Schlussfolgerung Metastasen in Knochen, Lunge und Lymphknoten erhöhen die Strahlenresistenz von Brustkrebs.

Schlüsselwörter Brustkrebs · Basaler Subtyp · Primärtumor · Metastatischer Krebs · Strahlenresistenz

Abbreviations

ATCC	American Type Culture Collection
BW	Body weight
D_{10}	10% Survival dose
DMF	Dose modifying factor
ER	Estrogen receptor
FBS	Fetal bovine serum
MCF7	Michigan Cancer Foundation-7
Pg	Progesterone receptor
SD	Standard deviations
T_D	Doubling time
TdT	Terminal deoxynucleotidyl transferase
TUNEL	Terminal deoxynucleotidyl transferase-mediated dUTP-biotin nick-end labeling

Introduction

Breast cancer is the most common cancer in women worldwide, with more than one million new cases diagnosed each year [1]. Breast cancer metastasizes primarily to the bone, lung, lymph nodes, liver and brain, and distant metastasis of this kind accounts for nearly 90% of deaths due to breast cancer. Therefore, strategies for its treatment need to be developed. Breast cancer represents a heterogeneous disease comprising several intrinsic subtypes with distinct clinical outcomes, such as basal-like, HER2-enriched, luminal A, luminal B, and normal-like [2–4]. Of these, the luminal A subtype carries the best prognosis with the lowest metastatic potential, whereas the basal subtype carries the poorest prognosis with the highest metastatic potential [1, 5, 6].

Several studies have thus far examined the ionizing radiation sensitivity of primary and metastatic cancer. Rantanen et al. found that the clonogenic survival after X-irradiation of UT-EC-2A (established from a patient with endometrial adenocarcinoma) is comparable to that of UT-EC-2B (established from the same patient but 17 months later from metastasis in the left supraclavicular fossa) [7]. Huerta et al. compared SW480 (established from a patient with primary colon adenocarcinoma) with SW620 (established from the same patient but 6 months later from a lymph node metastasis), and found that SW620 is more resistant to γ-induced apoptosis than SW480 [8, 9]. van den Aardweg et al. reported wide variations in clonogenic survival after X-irradiation among eight uveal melanoma cell lines (four primary and four metastatic from different patients) independently of whether or not a cell line is metastatic [10]. However, there have been no such reports for breast cancer.

Radiotherapy is used for metastasis from breast cancer [11–14], for which the dose is determined by considering the characteristics of the primary cancer based on clinical experience, but not that of metastatic cancer. Thus, we set out to establish the metastatic cell lines from the basal subtype cell line, and characterize the radiosensitivity of such metastatic cell lines.

Materials and methods

Cells and cell cultures

Human breast adenocarcinoma cell lines MDA-MB-231 (ATCC® HTB-26™) and MCF7 (ATCC® HTB-22™) were purchased from the American Type Culture Collection (ATCC, Manassas, VA). MDA-MB-231 is a triple-negative, basal subtype that was established from a pleural effusion in a 51-year-old Caucasian woman with a metastatic mammary carcinoma [15, 16]. MCF7 (Michigan Cancer Foundation-7) is an estrogen receptor (ER)-positive, progesterone receptor (PgR)-positive, luminal A-subtype that was established from a pleural effusion in a 69-year-old Caucasian woman with a metastatic mammary carcinoma [17, 18]. Unless otherwise specified, all cell cultures were maintained in RPMI1640 (R8758, Sigma-Aldrich, St Louis, MO) containing 10% fetal bovine serum (FBS) at 37°C in a humidified atmosphere of 5% CO_2 in air. For all the experiments, control cells were sham-manipulated and handled in parallel with the test cells.

Establishment of pGL4.5 cell line and its metastatic cell lines by in vivo selections

The pGL4.50[*luc2*/CMV/Hygro] vector (E1310, Promega, Madison, WI) encodes the luciferase reporter gene *luc2*, cytomegalovirus promoter and Hygromycin B resistance gene. MDA-MB-231 cells were lipofected with the pGL4.50[*luc2*/CMV/Hygro] vector using Lipofectamin2000 (Invitrogen, Carlsbad, CA), and were maintained in RPMI1640 containing 10% FBS and 0.1 mg/ml Hygromycin B (Life Technologies, Carlsbad, CA). The resulting cell line was named "pGL4.5" cells, which can be visualized with luciferase based, noninvasive bioluminescence imaging [19].

To obtain metastatic cell lines derived from pGL4.5 cells, 4- to 5-week old female BALB/cAJcl-*nu*/*nu* athymic nude mice purchased from CLEA Japan (Tokyo, Japan) were used. All animal experiments were approved by the Animal Experiments Committee of Fukushima Medical University (approval No. 2506), and conducted according to the guidelines of the committee. Mice were anesthetized via intraperitoneal injection of a mixture of medetomidine (0.2 μg/g body weight: BW), midazolam (2.2 μg/g BW) and butorphanol tartrate (2.8 μg/g BW).

To establish a cell line metastatic to the lymph nodes, pGL4.5 cells were orthotropically implanted into the mammary fat pad (Fig. S1). Briefly, with a 27-gauge needle, 1×10^6 pGL4.5 cells in 0.1 ml were inoculated in about 1 min into the mammary fat pad of anesthetized mice [20]. At 20–30 days after inoculation of pGL4.5 cells, D-Luciferin (in vivo grade VivoGlo™ Luciferin, Promega) was intraperitoneally injected into anesthetized mice at 150 μg/g BW. At 5 min after injection, metastatic lymph node lesions were visualized with bioluminescence imaging using the IVIS Lumina Imaging System (Xenogen Corporation, Alameda, CA), and isolated. Cells obtained from isolated lymph nodes were expanded in RPMI1640 containing 10% FBS, 0.1 mg/ml Hygromycin B, 200 U/ml penicillin and 200 μg/ml streptomycin, and the resulting cell line metastatic to the lymph nodes was named "NLN0001" cells (Fig. S2). Likewise, NLN0001 cells underwent the same orthotropic implantation procedures one more time, and the resulting cell line was named "NLN0104" cells (Fig. S2).

MDA-MB-231 cells form metastases in the bone, lung and elsewhere from the bloodstream when inoculated into the left cardiac ventricle of immunodeficient mice [21]. Therefore, to establish cell lines metastatic to the bone or lung, pGL4.5 cells were subjected to left ventricular cardiac injection (Fig. S1). In brief, after observing a back flow into the syringe, 1×10^5 pGL4.5 cells in 0.1 ml were inoculated with a 27-gauge needle in about 1 min into the left ventricle of anesthetized mice [19, 21]. With the same method as described for NLN0001 cells, metastatic bone or lung lesions were isolated, followed by expansion and reinoculation of cells. After repeating the left ventricular cardiac injections three times, the cell lines metastatic to the bone and lung were obtained and named "NBOS0042" and "NLU0041", respectively (Fig. S2). For more detailed information, see the legend to Fig. S2.

Table S1 shows the frequency of metastasis to the bone, lung and lymph nodes in pGL4.5 cells and its metastatic cell lines. Metastatic frequency was 0–50% in pGL4.5 cells, which was increased to 83% for the lymph nodes in NLN0001 cells established by the in vivo selection once. Moreover, metastatic frequency was 100% for the lymph nodes in NLN0104 cells established by the in vivo selection twice, as well as for the bone and lung in NBOS0042 and NLU0041, respectively, both of which were established by the in vivo selections three times.

Cell proliferation assay

For in vivo experiments, 1×10^6 cells were inoculated into each of six mammary glands (three on the left side and three on the right side) in 4- to 5-week old female BALB/cAJcl-*nu*/*nu* athymic nude mice. Tumor size was measured at 4–37 days after inoculation, and the tumor volume (mm^3) was calculated as $(\pi / 6) \times L \times W^2$, where L and W are the major and minor axial lengths in millimeters, respectively. For in vitro experiments, 3×10^4 cells were plated into each well of a 12-well plate. At every 24–196 h after plating, cells were counted using a Coulter Z-1 counter (Beckman Coulter, Fullerton, CA). Growth curves were fitted against the data for the tumor volume (in vivo) at 22–37 days after inoculation and the cell numbers (in vitro) at 24–120 h after plating to the exponential equation $y = a * \exp(b * x)$, where y is the tumor volume (mm^3) or the cell numbers, x is time in days for the tumor volume and in h for the cell numbers, a is intercept, and b is slope. Doubling time (T_D) in days for the tumor volume and h for the cell numbers was calculated as $\ln(2 / b)$.

Alamar Blue assay was also performed in vitro as described [22]. In brief, 3×10^3 cells were plated into each well of a 96-well plate. At every 24–120 h after plating, 10% Alamar Blue in PBS (Molecular Probes, Eugene, OR) was added, and cells were incubated at 37˚C/5% CO_2 for 4 h, followed by measurements of fluorescence with an excitation wavelength at 560 nm and an emission wavelength at 590 nm using a microplate reader (Varioskan® Flash, Thermo Fisher Scientific, Vantaa, Finland). For each cell line, the data for 48–120 h time points are shown as fold changes relative to the data for the 24 h time point.

Wound healing assay

A wound healing assay was conducted as described [23]. Briefly, 5×10^5 cells were plated into each well of a 12-well plate. At 24 h after plating, confluent cell monolayers were scrape-wounded with a 200 µl micropipette tip (H-110-96RS, QSP, Petaluma, CA). At 0, 4, 8 and 22 h after wounding, images were captured with an Olympus IX71 microscope equipped with an UPIan FLN10X/0.3 objective and DP2-BSW software. The distance between wound edges was measured in three randomly chosen regions for each sample. The percentage of wound closure was calculated as $100 \times (d_0 - d_t) / d_0$, where d_0 is the distance between wound edges at 0 h and d_t is that at 4, 8 or 22 h after wounding.

Matrigel invasion assay

A Matrigel invasion assay was carried out using BD BioCoat™ Matrigel™ Invasion Chamber (BD Biosciences, Bedford, MA) according to the manufacturer's instruction. In brief, for each well of a 24-well transwell chamber plate, 0.5 ml of RPMI1640 containing 1×10^4 cells but without FBS was added to the upper compartment, and 0.5 ml of RPMI1640 containing 5% FBS but without cells was added to the lower compartment. Chambers were incubated at 37˚C/5% CO_2 for 22 h. Invasive cells having passed through to the lower surface of the membrane filter were fixed with methanol, stained with 0.05% crystal violet (Wako, Osaka, Japan), and counted.

Clonogenic survival assay

Cell survival was determined by the clonogenic survival assay as described [24, 25]. Briefly, 5×10^4 cells were seeded onto a 3.5-cm dish at 2 days prior to irradiation. Cells were irradiated with single, graded doses of X-rays at room temperature from an X-ray generator (MBR-1520R-3, Hitachi Medico, Tokyo, Japan) operated at 150 kV and 20 mA with a 1 mm aluminum equivalent filter, at a source to surface distance of 40 cm and a dose rate of 4 Gy/min. Cultures were reseeded into 6-cm dishes in triplicate at 24 h after irradiation, and were incubated for 2 weeks, upon which cultures were fixed in methanol and stained with 0.05% crystal violet. Only colonies consisting of 50 or more cells were scored as survivors. Survival curves were fitted against the means of five or six independent experiments to the linear quadratic equation, predicated upon which the dose required to reduce the surviving fraction to 0.1 (10% survival dose, D_{10}) was determined. The dose modifying factor (DMF) was calculated as D_{10} for NBOS0042, NLU0041 or NLN0104 cells divided by that for pGL4.5 cells.

TUNEL assay

Apoptosis was detected by the terminal deoxynucleotidyl transferase (TdT)-mediated dUTP-biotin nick-end labeling (TUNEL) method, using the ApopTag® Peroxidase *In Situ* Apoptosis Detection kit (S7100, Chemicon International), as described [26]. In brief, 2×10^4 cells were plated onto a 1.2-cm-diameter round coverslip (Matsunami Glass, Osaka, Japan) at 2 days prior to irradiation. At every 24–120 h after irradiation with 6 Gy of X-rays at 4 Gy/min as aforementioned, cells were fixed on ice in 1% paraformaldehyde and permeabilized in 0.5% Triton X-100. After endogenous peroxidase was quenched with 3% hydrogen peroxide, the coverslips were reacted with TdT enzyme and peroxidase-conjugated anti-digoxigenin antibody. Positive TUNEL staining was developed with diaminobenzidine and indicated by a brown precipitate. The cells were counterstained with 0.5% methyl green, and viewed under an Olympus IX71 microscope after mounting. For each sample, 1000 or more cells were analyzed.

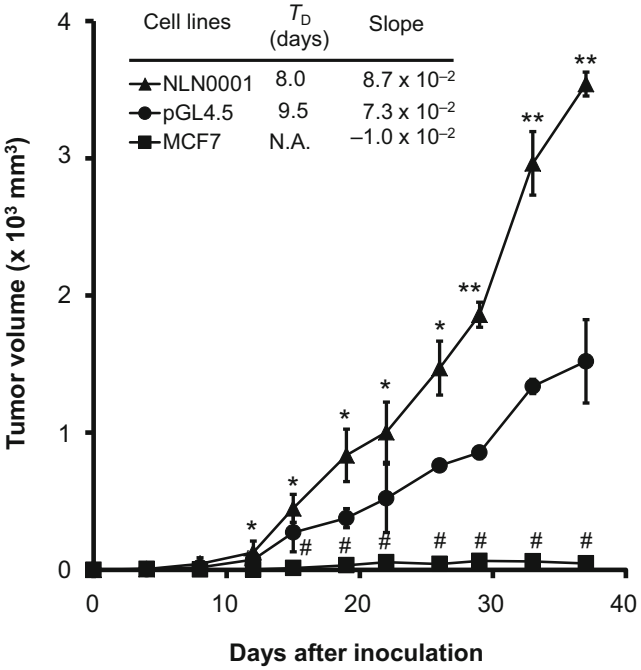

Fig. 1 Cell proliferation in vivo. Tumor volume (≥two mammary glands/mouse) was evaluated at 4–37 days after 1×10^6 cells (MCF7 [*filled squares*], pGL4.5 [*filled circles*] and NLN0001 [*filled triangles*] cells) were orthotropically inoculated into each of six mammary glands of athymic nude mice (three mice/*cell line*) (*$p < 0.05$, **$p < 0.005$ between NLN0001 and pGL4.5. #$p < 0.001$ between MCF7 and pGL4.5. Growth curves were fitted against the data for the tumor volume (mm^3) at 22–37 days after inoculation to the exponential equation $y = a * \exp(b * x)$, where y, x, a and b are the tumor volume (mm^3), time (days), intercept and slope, respectively. Doubling time (T_D) in days was calculated as $\ln(2 / b)$. *N.A.* not available)

Statistical analysis

All data were calculated as the means and standard deviations (SD) of three or more independent experiments. Statistical comparisons between groups were made by two-sample Student's *t*-test assuming unequal variances, and a p value of 0.05 or less was considered to be significant.

Results

Proliferation of metastatic cell lines is increased in vivo but not in vitro

The in vivo tumor growth of MCF7, pGL4.5 and NLN0001 cells was analyzed (Fig. 1). As expected, MCF7 cells that served as a negative control here did not grow significantly (e. g., $p = 0.35$ between 22 and 37 days after inoculation). In contrast, at ≥12 days after inoculation, pGL4.5 cells exhibited significant growth compared with MCF7 cells ($p < 0.001$), and growth of NLN0001 cells was significantly enhanced compared with pGL4.5 cells ($p < 0.02$). Next, the in vitro proliferation of pGL4.5, NBOS0042, NLU0041 and NLN0104 cells was evaluated with the two different methods, but there was no significant difference among cell lines (Fig. S3). These results indicate that metastatic cell lines possess an increased proliferative potential in vivo, but not in vitro.

Chemotaxis and invasion of metastatic cell lines are increased in vitro

Many studies have reported that metastatic cancer cells are more chemotactic and invasive than primary cancer cells [27–29]. Therefore, chemotaxis and invasion were assessed. The wound healing assay (Fig. 2) revealed that wound closure occurs in three metastatic cell lines (NBOS0042, NLU0041 and NLN0104 cells) significantly faster than in pGL4.5 cells at 4–22 h after wounding ($p < 0.03$), with no significant difference amongst three metastatic cell lines at 22 h after wounding ($p > 0.2$). A Matrigel invasion assay (Fig. 3) showed that the fraction of invasive cells was significantly higher in three metastatic cell lines compared with pGL4.5 cells ($p < 0.044$), without significant difference among three metastatic cell lines ($p > 0.67$). These results indicate that metastatic cell lines have an increased chemotactic (migratory) and invasive potential in vitro.

Metastatic cell lines are more radioresistant in vitro

The clonogenic survival assay (Fig. 4) revealed that three metastatic cell lines (NBOS0042, NLU0041 and NLN0104 cells) are more resistant to X-induced clonogenic inactivation than pGL4.5 cells ($p < 0.007$), with no significant difference amongst three metastatic cell lines ($p > 0.11$). DMF was 1.37, 1.39 and 1.32 for NBOS0042, NLU0041 and NLN0104 cells, respectively. TUNEL assay (Fig. 5) showed that three metastatic cell lines are more re-

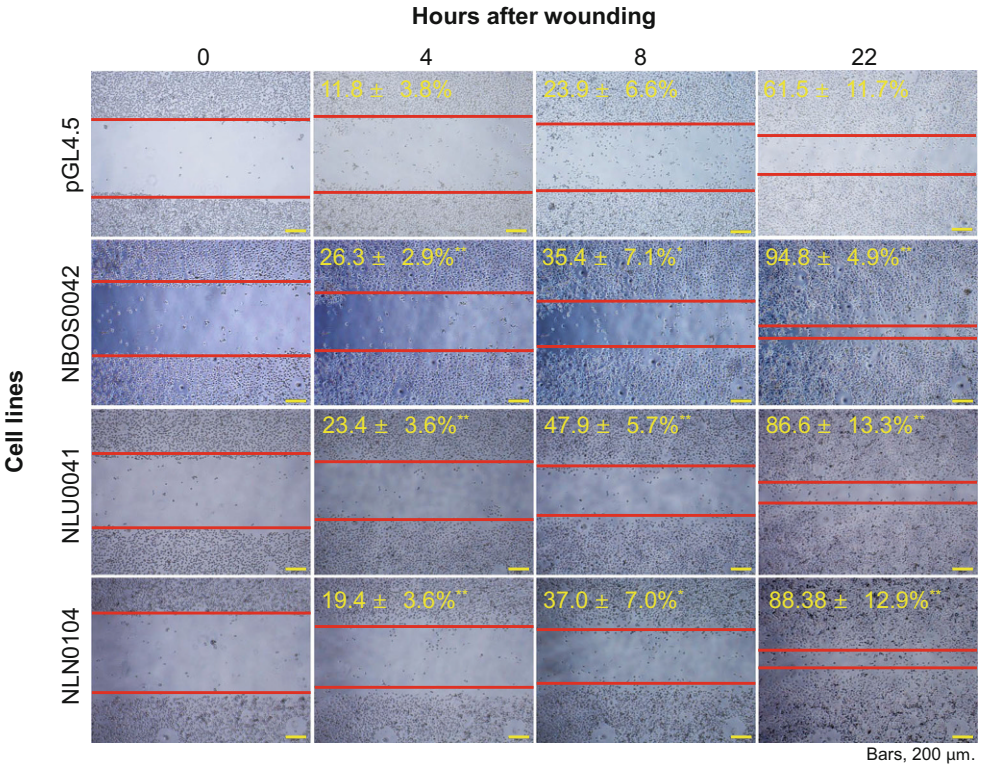

Fig. 2 Chemotaxis in vitro tested with a wound healing assay. Wound closure was assessed at 0, 4, 8 and 22 h after confluent monolayers of pGL4.5, NBOS0042, NLU0041 and NLN0104 cells were scrape-wounded. The distance between wound edges was measured in three randomly chosen regions for each sample, and the data represent the means and SD of three independent experiments with triplicate samples (*$p < 0.05$, **$p < 0.005$ vs pGL4.5 cells. Scale bars, 200 µm)

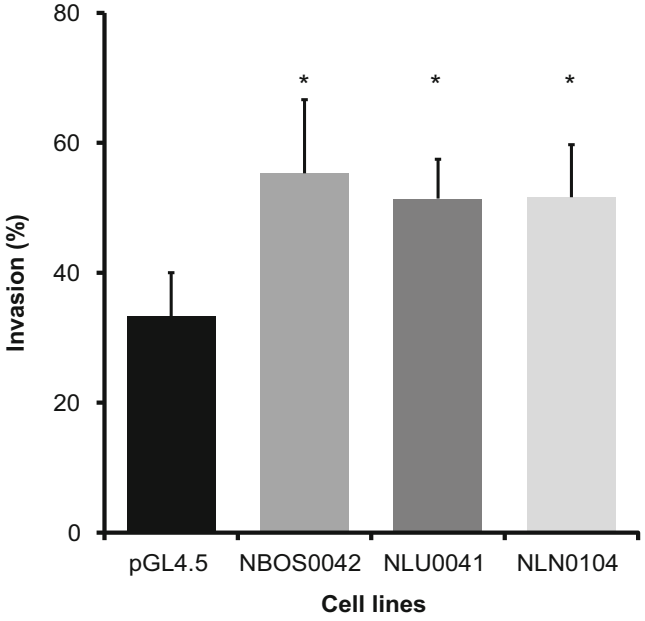

Fig. 3 Invasion in vitro tested with a Matrigel invasion assay. Invasive cells that migrated across a Matrigel-coated porous membrane for 22 h were counted in pGL4.5, NBOS0042, NLU0041 and NLN0104 cells. The data are presented as the means and SD of three to five independent experiments with triplicate or quadruplicate measurements (*$p < 0.05$ vs pGL4.5 cells)

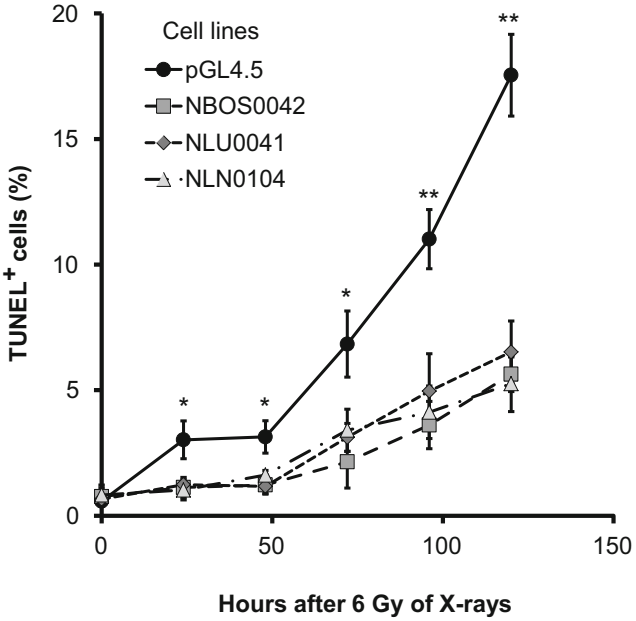

Fig. 5 Sensitivity to X-induced apoptosis in vitro determined with TUNEL assay. pGL4.5 (*circles*), NBOS0042 (*squares*), NLU0041 (*diamonds*) and NLN0104 (*triangles*) cells were fixed for TUNEL staining at every 24 h up to 120 h after irradiation with 6 Gy of X-rays. More than 1000 cells were analyzed for each sample, and the data are presented as the means and SD of three or four independent experiments with duplicate samples (*$p < 0.05$, **$p < 0.005$ vs NBOS0042, NLU0041 and NLN0104 cells)

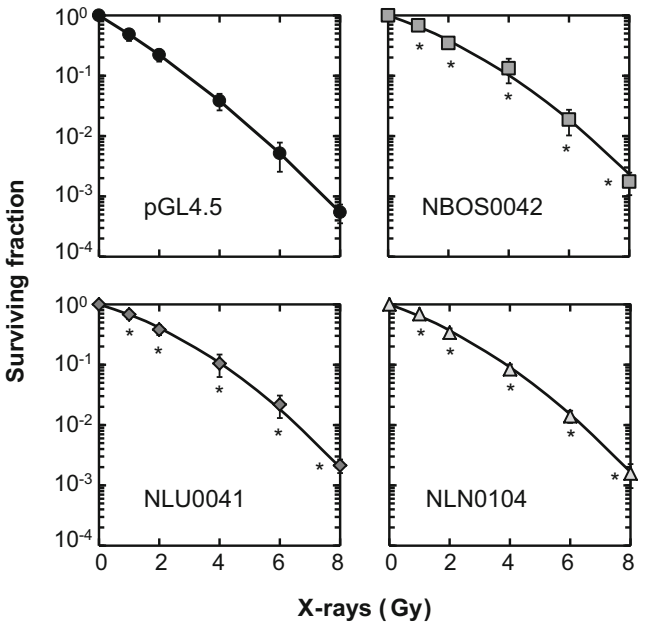

Fig. 4 Sensitivity to X-induced clonogenic inactivation in vitro determined with a clonogenic survival assay. pGL4.5 (*left upper panel*), NBOS0042 (*right upper panel*), NLU0041 (*left lower panel*) and NLN0104 (*right lower panel*) cells were replated for colony formation at 24 h after X-irradiation at indicated doses. The data represent the means and SD of five or six independent experiments with triplicate measurements (*$p < 0.01$ vs pGL4.5 cells)

sistant to X-induced apoptosis compared with pGL4.5 cells ($p < 0.04$), without significant difference amongst three metastatic cell lines ($p > 0.1$). These results indicate that metastatic cell lines are more radioresistant in vitro.

Discussion

Radiotherapy has been employed to treat metastasis. Whereas it is critical to understand the characteristics of metastatic cancer, the experimental animal model was unavailable that can compare the radiosensitivity of primary cancer and its metastatic counterpart. Here we have established a basal-like breast cancer cell line that can be visualized with bioluminescence imaging, and its derived cell lines that are highly metastatic to the bone, lung or lymph nodes by means of repetitive in vivo selections via orthotropic injections into the mammary fat pad or left ventricular cardiac injections (Table S1, Figs. S1 and S2). With this model, primary cancer and its metastatic counterpart can be compared directly both in vivo and in vitro. In addition, this model reflects more actual in vivo situations than other models, such as a bone metastasis model via a direct tumor implantation in bone or a lung metastasis model by tumor injection into a tail vein.

Our present data show that compared with pGL4.5 cells, NLN0001 cells have an increased proliferative potential in vivo (Fig. 1), and that the other three metastatic cell lines (NBOS0042, NLU0041 and NLN0104 cells) are more chemotactic (migratory), invasive, and resistant to X-induced clonogenic inactivation and apoptosis in vitro (Figs. 2, 3, 4 and 5).

A significantly increased proliferation observed in vivo in NLN0001 cells was not observed in vitro in other three metastatic cell lines (NBOS0042, NLU0041 and NLN0104 cells) (Fig. 1 and Fig. S3). In this regard, stromal cells are reported to promote angiogenesis and growth of human prostate tumors in a xenograft model [30], and human cancer-derived fibroblasts are known to stimulate proliferation and migration of human breast cancer cells via leptin signaling leading to increased tumor progression [31]. Such a supply of leptin, cytokines or other secretory factors from the tumor stroma that occurs in vivo does not occur in vitro, and this may account for our observed difference in vivo and in vitro. To test this possibility and further understand a different proliferative response observed in vitro and in vivo, proliferation in vitro (in the absence or presence of cytokines or other related secretory factors) and in vivo of NLN0001, NBOS0042, NLU0041 and NLN0104 cells needs to be tested.

Our in vitro analyses showed that three metastatic cell lines (NBOS0042, NLU0041 and NLN0104 cells) have increased radioresistance, which may be accounted for, at least in part, by resistance to radiogenic apoptosis (Figs. 4 and 5). Such apoptotic radioresistance was observed despite increased proliferation in vivo. In this respect, human Namalwa Burkitt lymphoma cells that received continuous proteasome inhibition with bortezomib are known to exhibit an apoptosis resistant and hyperproliferative phenotype, where an increase in Hsp27 and a decrease in p53 accompany such apoptosis resistance [32]. These warrant the in vivo validation experiments to irradiate tumors arising from our metastatic cell lines, analyze apoptosis in situ, and examine its underlying mechanisms in vitro.

Here we used only one basal subtype cell line (i. e., MDA-MB-231 cells) to establish pGL4.5 cells, and established more than ten metastatic cell lines each for the bone, lung and lymph nodes from pGL4.5 cells, from which we used only three metastatic cell lines (i. e., NBOS0042, NLU0041 and NLN0104 cells, respectively) to minimize the number of mice subjected to experiments and due to limited manpower. However, further characterization of several metastatic cell lines other than NBOS0042, NLU0041 and NLN0104 cells, as well as the use of several basal subtype cell lines other than MDA-MB-231 cells, to establish independent metastatic cell lines will be important to generalize our present findings, warranting further studies.

Acknowledgements The authors are indebted to Dr. Soile Tapio and Ms. Daniela Hladik (Helmholtz Zentrum München, Munich, Germany) for their help in the German translation of the abstract.

Funding This work was supported in part by a Grant-in-Aid for Scientific Research C (No. 23591844) from the Ministry of Education, Culture, Sports, Science and Technology (MEXT) of Japan.

Conflict of interest T. Hara, M. Iwadate, K. Tachibana, S. Waguri, S. Takenoshita and N. Hamada declare that they have no competing interests.

References

1. Blows FM, Driver KE, Schmidt MK et al (2010) Subtyping of breast cancer by immunohistochemistry to investigate a relationship between subtype and short and long term survival: a collaborative analysis of data for 10,159 cases from 12 studies. PLoS Med 7:e1000279
2. Perou CM, Sorlie T, Eisen MB et al (2000) Molecular portraits of human breast tumours. Nature 406:747–752
3. Rouzier R, Perou CM, Symmans WF et al (2005) Breast cancer molecular subtypes respond differently to preoperative chemotherapy. Clin Cancer Res 11:5678–5685
4. van't Veer LJ, Dai H, van de Vijver MJ et al (2002) Gene expression profiling predicts clinical outcome of breast cancer. Nature 415:530–536
5. Rodriguez-Pinilla SM, Sarrio D, Honrado E et al (2006) Prognostic significance of basal-like phenotype and fascin expression in node-negative invasive breast carcinomas. Clin Cancer Res 12:1533–1539
6. Nalwoga H, Arnes JB, Wabinga H, Akslen LA (2010) Expression of aldehyde dehydrogenase 1 (ALDH1) is associated with basal-like markers and features of aggressive tumours in African breast cancer. Br J Cancer 102:369–375
7. Rantanen V, Grénman S, Kulmala J, Jaakkola M, Lakkala T, Sajantila A et al (1995) Characterization and radiosensitivity of UT-EC-2A and UT-EC-2B, two new highly radiosensitive endometrial cancer cell lines derived from a primary and metastatic tumor of the same patient. Gynecol Oncol 56:53–62
8. Huerta S, Heinzerling JH, Anguiano-Hernandez YM et al (2007) Modification of gene products involved in resistance to apoptosis in metastatic colon cancer cells: roles of Fas, Apaf-1, NFkappaB, IAPs, Smac/DIABLO, and AIF. J Surg Res 142:184–194
9. Cai K, Mulatz K, Ard R, Nguyen T, Gee SH (2014) Increased diacylglycerol kinase ζ expression in human metastatic colon cancer cells augments Rho GTPase activity and contributes to enhanced invasion. BMC Cancer 14:208
10. van den Aardweg GJ, Naus NC, Verhoeven AC, de Klein A, Luyten GP (2002) Cellular radiosensitivity of primary and metastatic human uveal melanoma cell lines. Invest Ophthalmol Vis Sci 43:2561–2565
11. Feyer PC, Steingraeber M (2012) Radiotherapy of bone metastasis in breast cancer patients – current approaches. Breast Care 7:108–112
12. Jaboin JJ, Ferraro DJ, DeWees TA et al (2013) Survival following gamma knife radiosurgery for brain metastasis from breast cancer. Radiat Oncol 8:131
13. Lee SS, Ahn JH, Kim MK et al (2008) Brain metastases in breast cancer: prognostic factors and management. Breast Cancer Res Treat 111:523–530
14. Steinauer K, Gross MW, Huang DJ, Eppenberger-Castori S, Guth U (2014) Radiotherapy in patients with distant metastatic breast cancer. Radiat Oncol 9:126

15. Cailleau R, Young R, Olive M, Reeves WJ Jr (1974) Breast tumor cell lines from pleural effusions. J Natl Cancer Inst 53:661–674
16. Camp JT, Elloumi F, Roman-Perez E et al (2011) Interactions with fibroblasts are distinct in basal-like and luminal breast cancers. Mol. Cancer Res 9:3–13
17. Brooks SC, Locke ER, Soule HD (1973) Estrogen receptor in a human cell line (MCF-7) from breast carcinoma. J Biol Chem 248:6251–6253
18. Subik K, Lee JF, Baxter L et al (2010) The expression patterns of ER, PR, HER2, CK5/6, EGFR, Ki-67 and AR by immunohistochemical analysis in breast cancer cell lines. Breast Cancer 4:35–41
19. Minn AJ, Kang Y, Serganova I et al (2005) Distinct organ-specific metastatic potential of individual breast cancer cells and primary tumors. J Clin Invest 115:44–55
20. Hackl C, Man S, Francia G, Milsom C, Xu P, Kerbel RS (2013) Metronomic oral topotecan prolongs survival and reduces liver metastasis in improved preclinical orthotopic and adjuvant therapy colon cancer models. Gut 62:259–271
21. Kang Y, Siegel PM, Shu W et al (2003) A multigenic program mediating breast cancer metastasis to bone. Cancer Cell 3:537–549
22. Al-Nasiry S, Geusens N, Hanssens M, Luyten C, Pijnenborg R (2007) The use of alamar blue assay for quantitative analysis of viability, migration and invasion of choriocarcinoma cells. Hum Reprod 22:1304–1309
23. Riou P, Saffroy R, Chenailler C et al (2006) Expression of T-cadherin in tumor cells influences invasive potential of human hepatocellular carcinoma. FASEB J 20:2291–2301
24. Hamada N, Hara T, Omura-Minamisawa M et al (2008) The survival of heavy ion-irradiated Bcl-2 overexpressing radioresistant tumor cells and their progeny. Cancer Lett 268:76–81
25. Hara T, Omura-Minamisawa M, Kang Y, Cheng C, Inoue T (2008) Flavopiridol potentiates the cytotoxic effects of radiation in radioresistant tumor cells in which p53 is mutated or Bcl-2 is overexpressed. Int J Radiat Oncol Biol Phys 71:1485–1495
26. Hamada N, Ni M, Funayama T, Sakashita T, Kobayashi Y (2008) Temporally distinct response of irradiated normal human fibroblasts and their bystander cells to energetic heavy ions. Mutat Res 639:35–44
27. Chen J, Gallo KA (2012) MLK3 regulates paxillin phosphorylation in chemokine-mediated breast cancer cell migration and invasion to drive metastasis. Cancer Res 72:4130–4140
28. Luker KE, Luker GD (2006) Functions of CXCL12 and CXCR4 in breast cancer. Cancer Lett 238:30–41
29. Banyard J, Chung I, Migliozzi M et al (2014) Identification of genes regulating migration and invasion using a new model of metastatic prostate cancer. BMC Cancer 14:387
30. Tuxhorn JA, McAlhany SJ, Dang TD, Ayala GE, Rowley DR (2002) Stromal cells promote angiogenesis and growth of human prostate tumors in a differential reactive stroma (DRS) xenograft model. Cancer Res 62:3298–3307
31. Barone I, Catalano S, Gelsomino L et al (2012) Leptin mediates tumor-stromal interactions that promote the invasive growth of breast cancer cells. Cancer Res 72:1416–1427
32. Domink F, Carsten B, Gerhard O, Volker D, Naujokat C (2008) Increased expression and altered subunit composition of proteasomes induced by continuous proteasome inhibition establish apoptosis resistance and hyperproliferation of Burkitt lymphoma cells. J Cell Biochem 10:270–283